Optical Fibers and Their Biomedical Applications

Govind P. Agrawal

The Institute of Optics
University of Rochester
Rochester, New York, USA

Introduction

- Optical Fibers have found a variety of applications.
- High-capacity fiber-Optic links installed around the world make the magic of Internet and Telecommunications possible.
- Biomedical applications of fibers are increasing with the advent of photonic crystal and other microstructured fibers.
- Fibers act as optical wires and transport light just as electrical wires transport electricity.
- Nonlinear effects inside fibers provide a variety of new applications.
- This seminar provides a general overview of optical fibers with emphasis on their biomedical applications.
- Physical mechanism behind optical fibers: Total Internal Reflection (TIR).

Historical Evolution

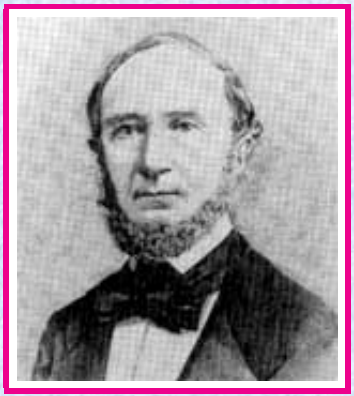

Daniel Colladon

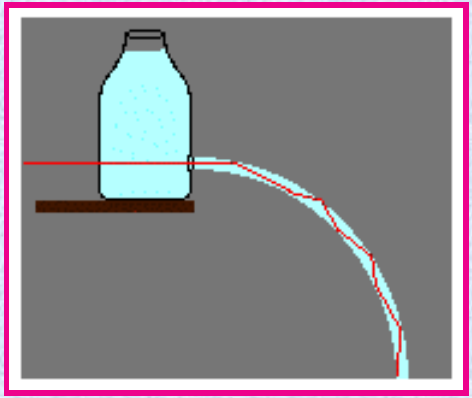

Experimental Setup

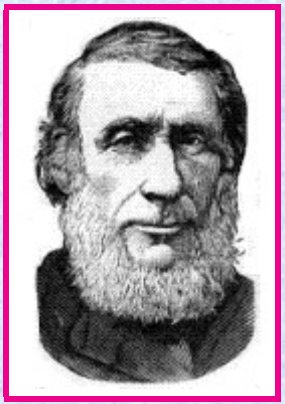

John Tyndall

- TIR is attributed to John Tyndall (1854 experiment in London).
- The book *City of Light* by Jeff Hecht (1999) traces history of TIR.
- First demonstration in Geneva in 1841 by Daniel Colladon (Comptes Rendus, vol. 15, pp. 800-802, Oct. 24, 1842).
- Light remained confined to a falling stream of water.

Historical Details

- Tyndall repeated the experiment in a 1854 lecture at the suggestion of Faraday (but Faraday could not recall the original name).
- Tyndall's name got attached to TIR because he described the experiment in his popular book *Light and Electricity* (around 1860).
- Colladon published an article The Colladon Fountain in 1884 to claim credit but it didn't work (La Nature, Scientific American).

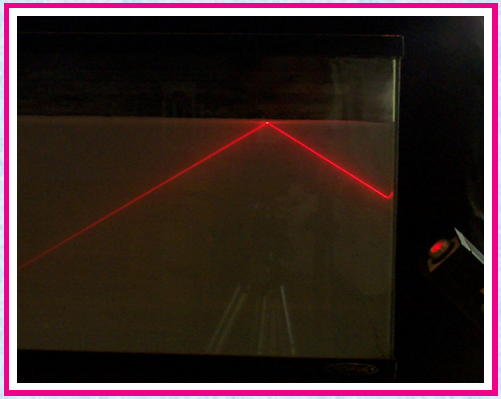

A fish tank and a laser pointer can be used to demonstrate the phenomenon of total internal reflection.

Early TIR Applications

- Luminous fountains used TIR during the "Exposition Universel" in Paris in November 1889.
- Photograph from La Nature, published in 1889 (Fig. 3 on p. 593)

Total Internal Reflection

- Refraction of light at a dielectric interface is governed by Snell's law: $n_1 \sin\theta_i = n_2 \sin\theta_t$ (around 1620).
- When $n_1 > n_2$, light bends away from the normal ($\theta_t > \theta_i$).
- At a critical angle $\theta_i = \theta_c$, θ_t becomes 90° (parallel to interface).
- Total internal reflection occurs for $\theta_i > \theta_c$.

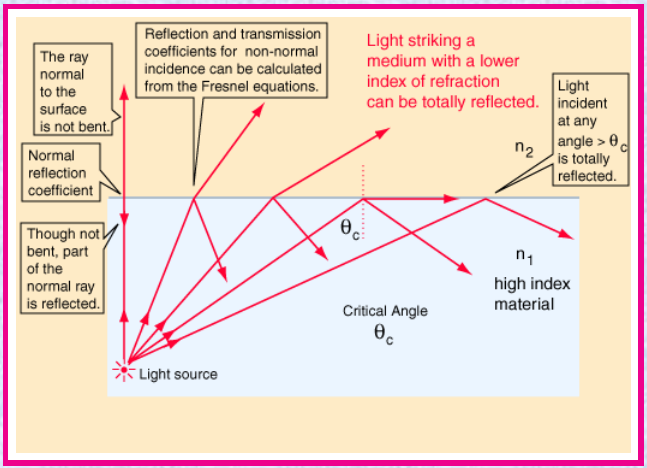

Cladded Glass Fibers

- Unclad glass fibers (diameter $<$1 mm) were made during 1920s.
- A fiber bundle for transmitting images patented by C. W. Hansell and used by H. Lamm of Germany in 1930.
- Bare glass fibers suffered from several practical issues.
- Van Heel in Holland coated glass fibers with silver but no light emerged from them (because of losses during multiple reflections).
- Brian O'Brien (Univ. of Rochester) suggested to van Heel the use of dielectric cladding in October 1951.
- By April 1952, Van Heel transmitted images over 50 cm using a bundle of 400 glass fibers with plastic cladding.

Early Fiber Applications

- Hirschowitz wanted to use optical fibers for making a flexible gastroscope in 1954.
- Glass cladding was used in 1956 by L. Curtiss at Univ. of Michigan.
- He used a glass rod inside a glass tube of lower refractive index.
- Such a fiber was used to build a gastroscope in Feb. 1957.
- First commercial fiber gastroscope became available in 1960 and soon after it was adopted by hospitals worldwide.
- Other early applications included cystocopes, image processing, and toys. Losses limited fiber lengths to a few meters.
- Narinder Kapany popularized fiber optics with his 1960 Scientific American article, followed with a book.

Modern Optical Fibers

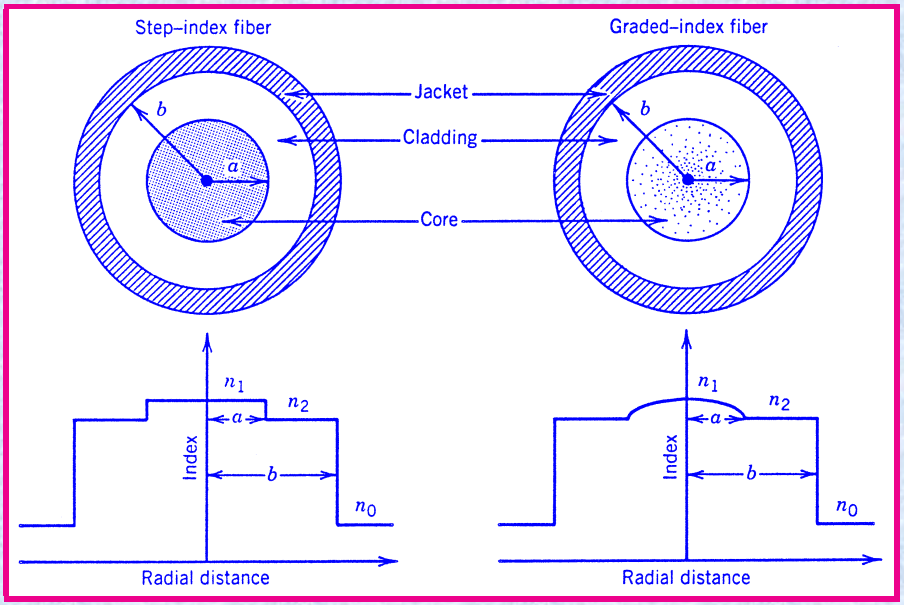

- Contain a central core surrounded by a lower-index cladding
- Two-dimensional waveguides with cylindrical symmetry
- Graded-index fibers: Refractive index varies inside the core.

Fiber Design

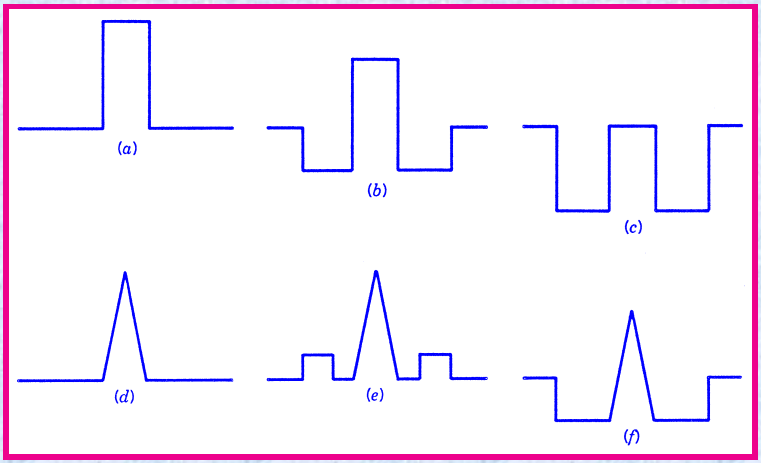

- Core doped with GeO_2; cladding with fluorine.
- Index profile rectangular for standard fibers.
- Triangular index profile for dispersion-shifted fibers.
- Raised or depressed cladding for dispersion control.




Silica Fibers

Two-Stage Fabrication

- **Preform:** Length 1 m, diameter 2 cm; correct index profile.
- Preform is drawn into fiber using a draw tower.

Preform Fabrication Techniques

- Modified chemical vapor deposition (MCVD).
- Outside vapor deposition (OVD).
- Vapor Axial deposition (VAD).

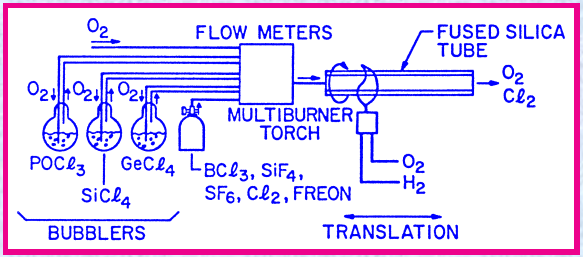

Fiber Draw Tower

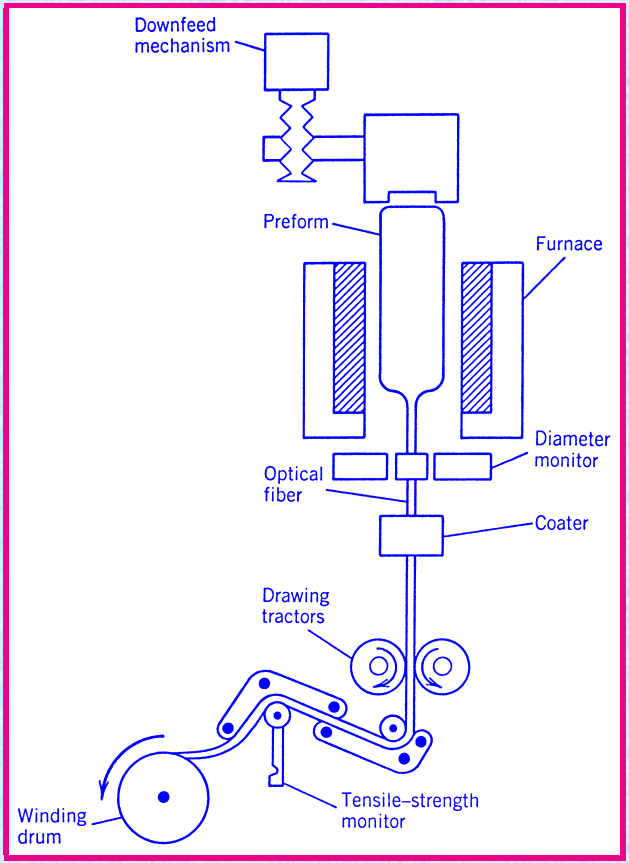

Fiber Properties

- Light guided over long lengths through total internal reflection.
- Propagation within the fiber depends on the number of modes supported by that fiber.
- One must solve Maxwell's equations to find these spatial modes.
- Important fiber parameter: $V = (2\pi/\lambda)a\sqrt{n_1^2 - n_2^2}$.
- Each mode has an effective refractive index: $n_2 < \bar{n} < n_1$.
- Only a single guided mode exists in fibers designed with $V < 2.4$.
- Typically $a = 5$ μm for $\lambda > 1.3$ μm for single-mode fibers.
- Nonlinear effects are enhanced in narrow-core fibers because of a reduced effective mode area.




Fiber Losses

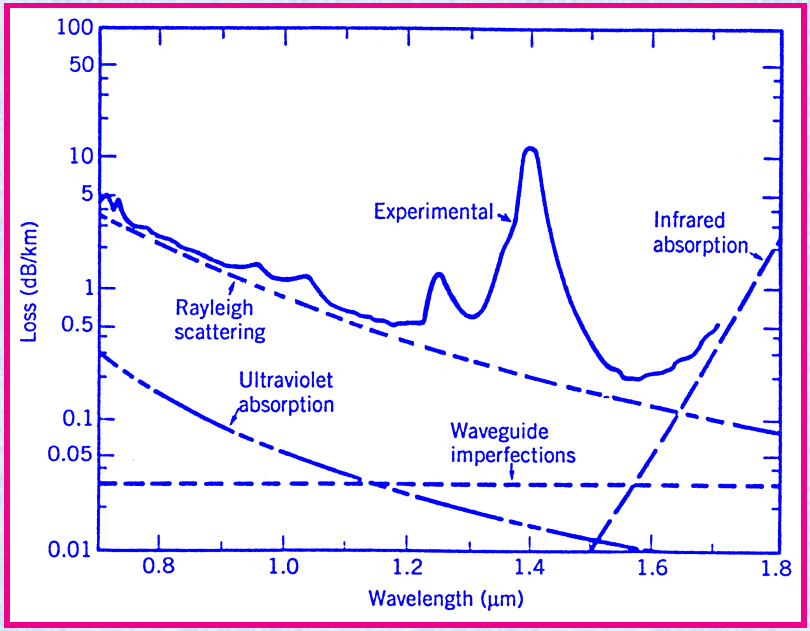

Definition: $P_{\text{out}} = P_{\text{in}} \exp(-\alpha L), \quad \alpha\ (\text{dB/km}) = 4.343\alpha.$

- Water peak near 1400 nm reduced considerably in modern fibers.
- Rayleigh scattering is the dominant loss mechanism (varies as λ^{-4})

Fiber Dispersion

- Origin: Frequency dependence of the mode index $\bar{n}(\omega)$:

$$\beta(\omega) = \bar{n}(\omega)\omega/c = \beta_0 + \beta_1(\omega - \omega_0) + \tfrac{1}{2}\beta_2(\omega - \omega_0)^2 + \cdots,$$

  where ω_0 is the carrier frequency of optical pulse.

- *Transit time* for a fiber of length L: $T = L/v_g = L(d\beta/d\omega)$.

- Different frequency components travel at different speeds and arrive at different times at output end (pulse broadening).

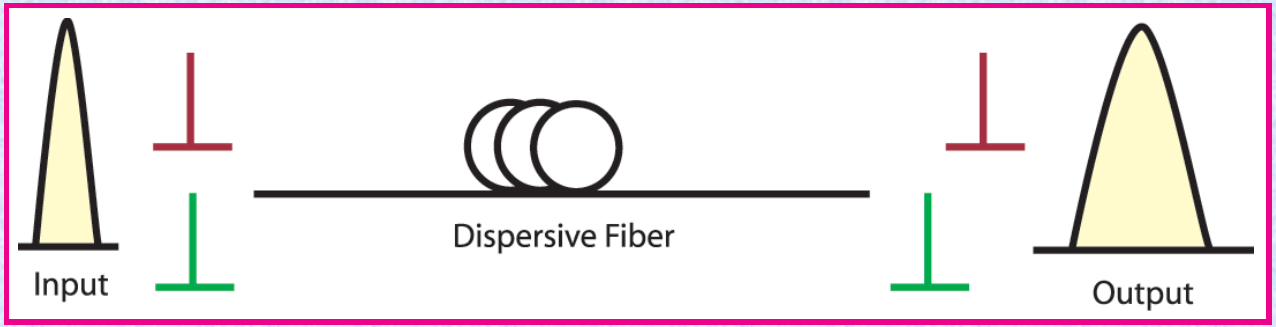

Fiber Dispersion

- Pulse broadening governed by group-velocity dispersion:

$$\Delta T = \frac{dT}{d\omega}\Delta\omega = \frac{d}{d\omega}\left(\frac{L}{v_g}\right) = L\beta_2\Delta\omega,$$

  $\Delta\omega$ is pulse bandwidth and L is fiber length.

- Second-order dispersion: $\beta_2 = \frac{d}{d\omega}\left(\frac{1}{v_g}\right) = \frac{d^2\beta}{d\omega^2}$ $(\mathrm{ps}^2/\mathrm{km})$

- Alternate definition: $D = \frac{d}{d\lambda}\left(\frac{1}{v_g}\right) = -\frac{2\pi c}{\lambda^2}\beta_2$ $(\mathrm{ps/km/nm})$

- Third-order Dispersion, governed by β_3, becomes important for femtosecond pulses. It is related to dispersion slope $\frac{dD}{d\lambda}$.

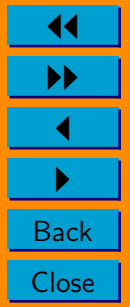

Waveguide Dispersion

- Mode index $\bar{n}(\omega) = n_1(\omega) - \delta n_W(\omega)$.
- Material dispersion D_M results from $n_1(\omega)$ (index of silica).
- Waveguide dispersion D_W results from $\delta n_W(\omega)$ and depends on core size and dopant distribution.
- Total dispersion $D = D_M + D_W$ can be controlled.

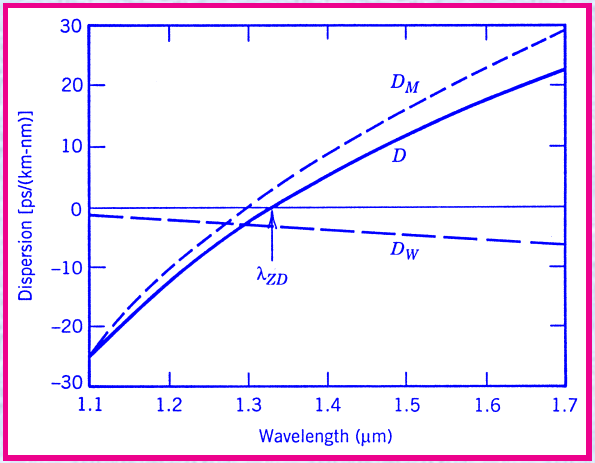

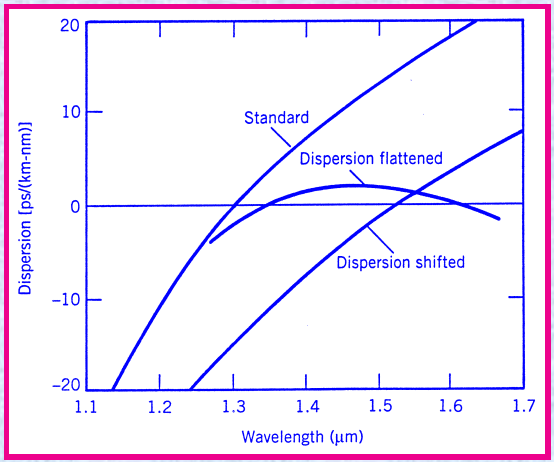

Major Nonlinear Effects

- Self-Phase Modulation (SPM)
- Cross-Phase Modulation (XPM)
- Four-Wave Mixing (FWM)
- Stimulated Brillouin Scattering (SBS)
- Stimulated Raman Scattering (SRS)

Origin of Nonlinear Effects in Optical Fibers

- Third-order nonlinear susceptibility $\chi^{(3)}$.
- Real part leads to SPM, XPM, and FWM.
- Imaginary part leads to SBS and SRS.

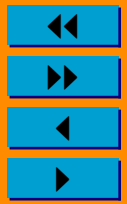

Self-Phase Modulation (SPM)

- Refractive index depends on intensity as

$$n(I) = n + n_2 I(t).$$

- $n_2 = 2.6 \times 10^{-20}$ m^2/W for silica fibers.
- Propagation constant: $\beta' = \beta + k_0 \bar{n}_2 (P/A_{\text{eff}}) \equiv \beta + \gamma P.$
- Nonlinear parameter: $\gamma = 2\pi \bar{n}_2 / (A_{\text{eff}} \lambda).$
- Nonlinear Phase shift:

$$\phi_{\text{NL}} = \int_0^L \gamma P_0 e^{-\alpha z} dz = \gamma P_0 L_{\text{eff}}, \quad L_{\text{eff}} = (1 - e^{-\alpha L})/\alpha.$$

- Optical field modifies its own phase (SPM).
- SPM leads to spectral broadening of optical pulses.

Nonlinear Schrödinger Equation

- Dispersive and Nonlinear effects are studied by solving a simple equation derived from Maxwell's equations.
- This equation is known as the Nonlinear Schrödinger Equation:

$$\frac{\partial A}{\partial z} + \frac{i\beta_2}{2}\frac{\partial^2 A}{\partial t^2} = i\gamma|A|^2 A - \frac{\alpha}{2}A.$$

- Nonlinear parameter: $\gamma = 2\pi\bar{n}_2/(A_{\text{eff}}\lambda)$.
- Fibers with large A_{eff} are useful for telecommunications.
- Highly nonlinear fibers are made with reduced A_{eff}.
- Nonlinear effects are enhanced considerably in photonic crystal and other microstructured fibers.

Cross-Phase Modulation (XPM)

- Refractive index seen by one wave depends on the intensity of other co-propagating waves.
- Nonlinear phase shifts for two waves take the form

$$\phi_a^{\mathrm{NL}} = \gamma_a L_{\mathrm{eff}}(P_a + 2P_b), \qquad \phi_b^{\mathrm{NL}} = \gamma_b L_{\mathrm{eff}}(P_b + 2P_a).$$

- The second term with a factor of 2 is due to XPM.
- Mathematically, XPM effects are governed by two coupled NLS equations.
- XPM is beneficial for applications such as optical switching, wavelength conversion, etc.
- XPM is a limiting factor for modern telecommunication systems.

Four-Wave Mixing

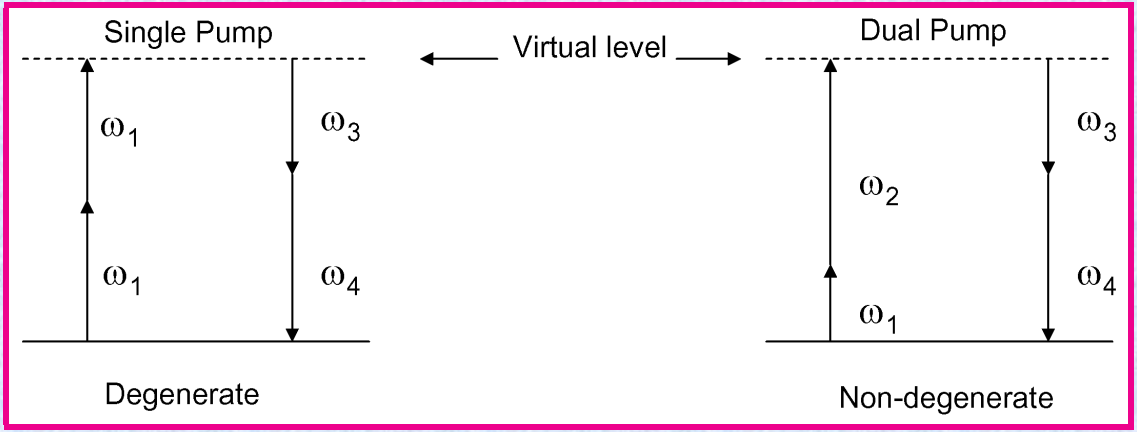

- FWM converts two photons from one or two pump beams into two new frequency-shifted photons.
- Energy conservation: $\hbar\omega_1 + \hbar\omega_2 = \hbar\omega_3 + \hbar\omega_4$.
- Momentum conservation leads to phase-matching condition.
- Useful for parametric amplification and wavelength conversion.

Brillouin Scattering

- Scattering of light from acoustic waves (electrostriction).
- Energy and momentum conservation laws require $\Omega_A = \omega_p - \omega_s$ and $\mathbf{k}_A = \mathbf{k}_p - \mathbf{k}_s$.
- Becomes a stimulated process at high input power levels.
- Most of power reflected once threshold is reached ($<$10 mW for fiber lengths $>$10 km).
- Brillouin gain has a narrow Lorentzian spectrum ($\Delta\nu \sim 20$ MHz).

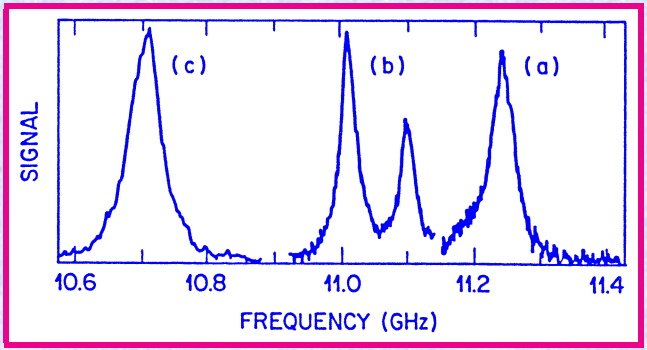

Stimulated Raman Scattering

- Scattering of light from vibrating molecules.
- Scattered light shifted in frequency.
- Raman gain spectrum extends over 40 THz.
- Raman shift at Gain peak: $\Omega_R = \omega_p - \omega_s \sim 13$ THz).

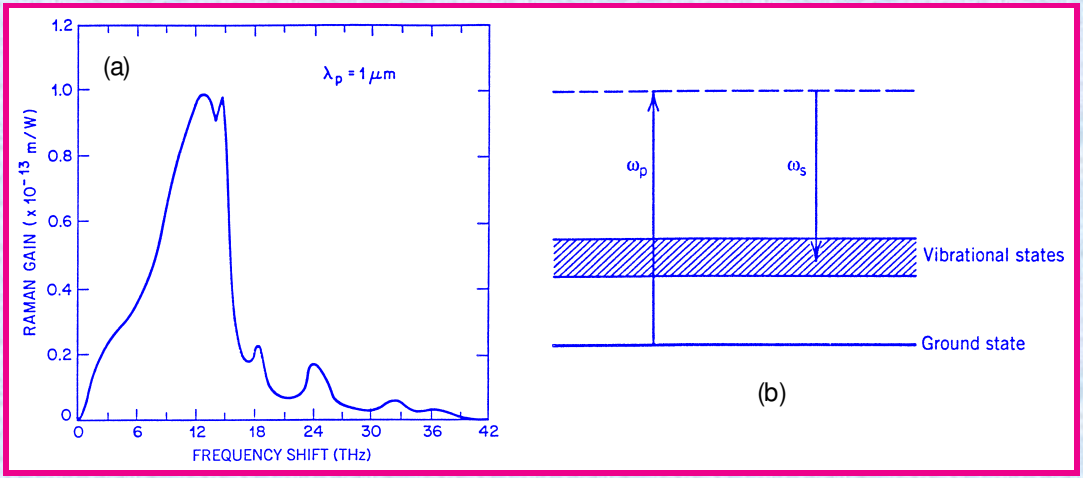

Microstructured Fibers

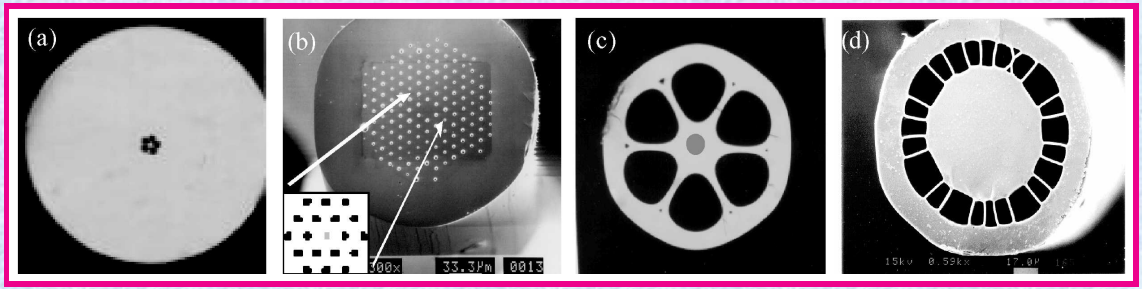

(Eggleton et al, Opt. Exp.**9**, 698, 2001)

- A narrow core is surrounded by a silica cladding with air holes.
- Photonic crystal fibers have multiple rings of holes.
- Number of air holes varies from structure to structure.
- Hole size varies from 0.5 to 5 μm depending on the design.
- Nonlinear effects are enhanced considerably (highly nonlinear fibers).
- Useful for supercontinuum generation among other things.

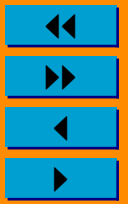

Back
Close

Supercontinuum Generation

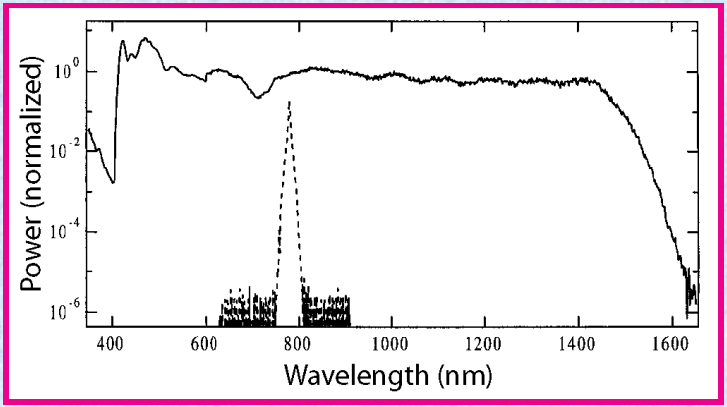

(Ranka et al., Opt. Lett. **25**, 25, 2000)

- Output spectrum generated in a 75-cm section of microstructured fiber using 100-fs pules with 0.8 pJ energy.
- Supercontinuum extends from 400 to 1600 nm.
- It is also relatively flat over the entire bandwidth.
- Useful in biomedical imaging as a broadband source.

Dispersion-Tailored Fibers

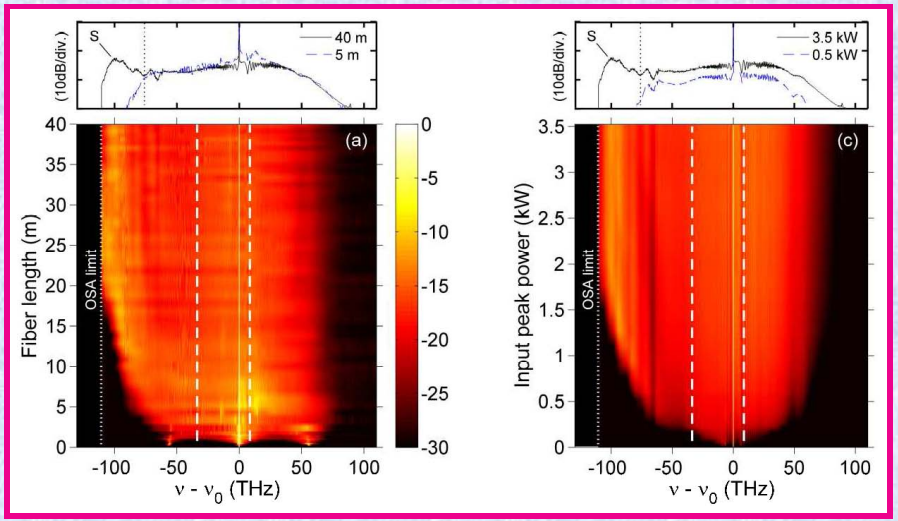

(Barviau et al., Opt. Exp. **17**, 7392, 2009)

- SC spectra as a function of fiber length and input peak power.
- A PCF with two zero-dispersion wavelengths was employed.
- Supercontinuum is relatively flat over the entire bandwidth.

Tapered Photonic Crystal Fibers

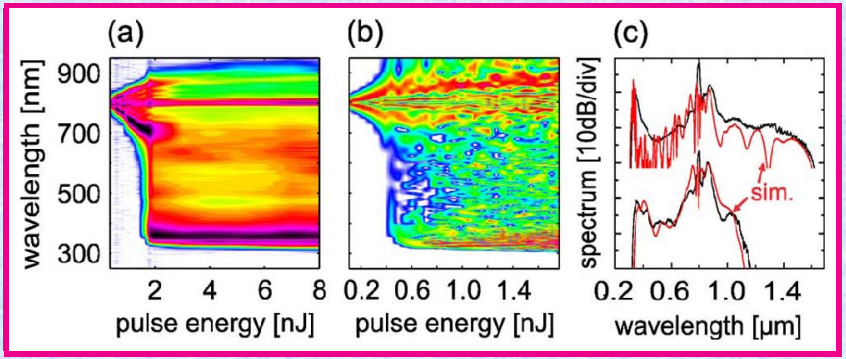

(Stark et al., Opt. Lett. **37**, 770, 2012)

- Experimental (a) and simulated (b) SC spectra when 110-fs pulses launched into a tapered PCF.
- (c) SC spectra at input pulse energies of 2 and 5 nJ.
- Core diameter tapered form 4.5 μm to 0.6 μm over 1 cm.
- Tapering helps to extend the supercontinuum into the UV region.

Supercontinuum-Based Biomedical Imaging

- Several companies sell fiber-based supercontinuum sources (NKT Photonics, Fianium, Koheras, Leukos, etc.].
- This has led to their use in biomedical imaging.
- Imaging techniques are known by a variety of names.
- I focus on 3 techniques: CARS microscopy; STED microscopy; optical coherence tomography.

CARS Nonlinear Process

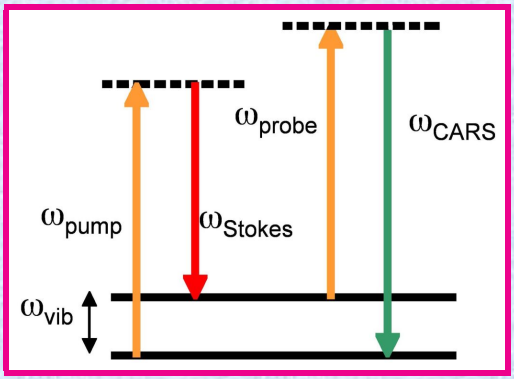

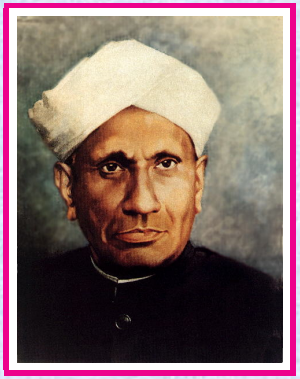

- Coherent anti-Stokes Raman scattering (CARS) is a well-known nonlinear process (Maker and Terhune, Phys. Rev., 1965).
- Pump and Stokes beam at ω_p and ω_s drive coherently a vibrational resonance at the frequency $\omega_{\text{vib}} = \omega_p - \omega_s$ (optical phonons).
- CARS signal generated at $\omega_{\text{CARS}} = 2\omega_p - \omega_s$.
- CARS is a kind of Raman-enhanced four-wave mixing process.

CARS Microscopy

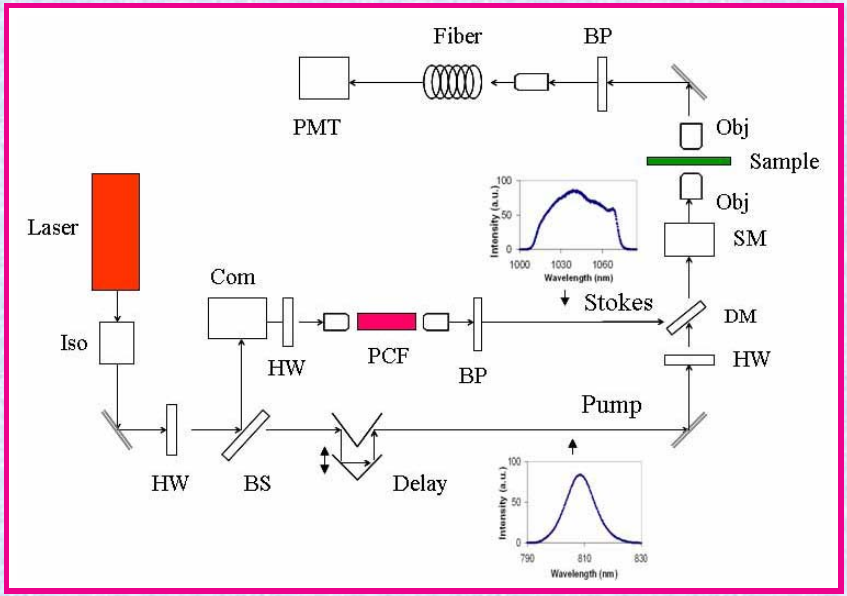

(Murugkar et al., Opt. Exp. **15**, 14028, 2007)

Laser pulses (65-fs) split to produce pump and Stokes beams.

Bandpass filter after the PCF selects the Stokes bandwidth.

Different Stokes frequencies excite different molecules in sample.

CARS Microscopy

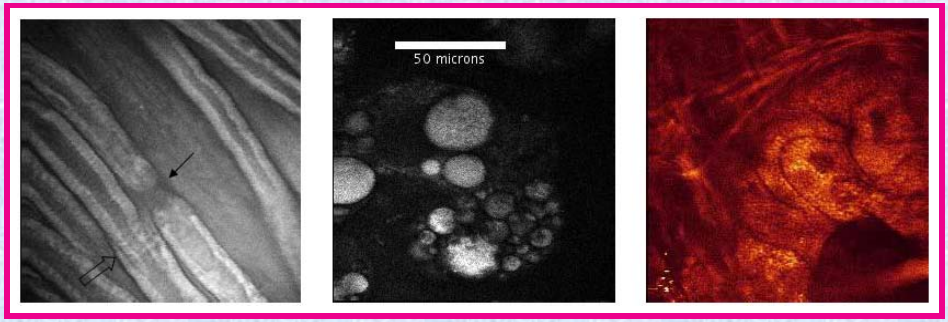

(Murugkar et al., Opt. Exp. **15**, 14028, 2007)

- Stokes pulses, broadened spectrally using a PCF, are sent to the sample together with pump pulses.
- Anti-Stokes signal generated inside the sample is used for microscopy.
- (a) Live rat dorsal root axon; (b) lipid droplets in a cell culture; (c) sebaceous gland in a mouse ear.
- Resolution is typically limited to 2-3 μm.

STED Microscopy

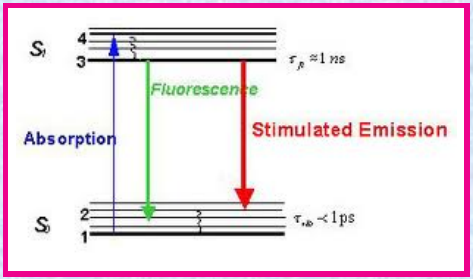

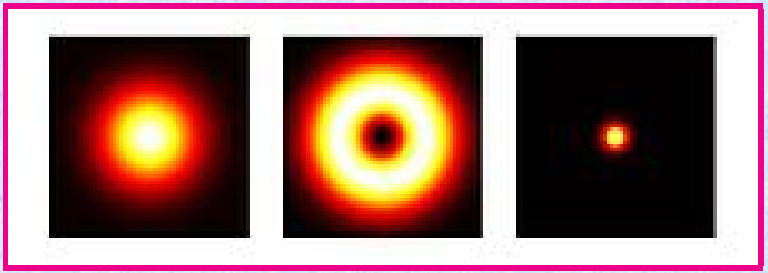

- Stimulated-emission depletion (STED) microscopy was first proposed in 1994 (Hell and Wichmann, Opt. Lett. **19**, 780, 1994).
- Fluorescence is suppressed in the off-center region using a second beam that removes excited molecules through stimulated emission.
- Nanoscale resolution ($\lambda/50$) realized by 2005 using a doughnut-shape STED pulsed beam.
- A fiber-based supercontinuum source was used by 2008.




Back
Close

STED Setup

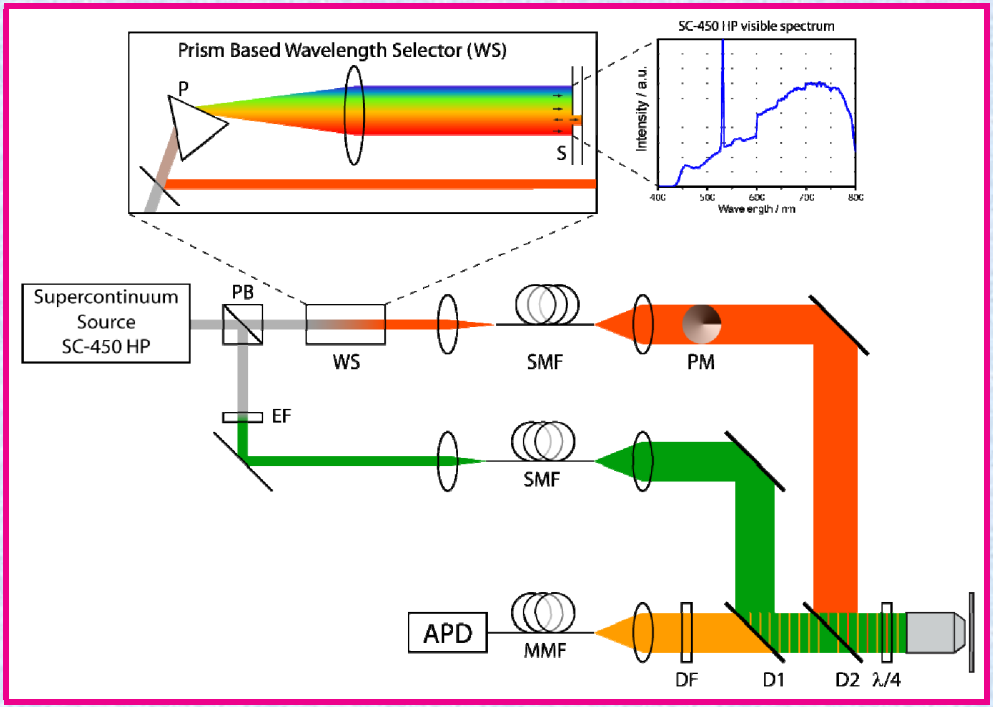

(Wildanger et al., Opt. Exp. **16**, 9614, 2008)

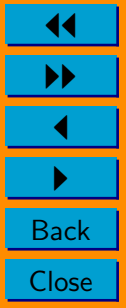

STED Results

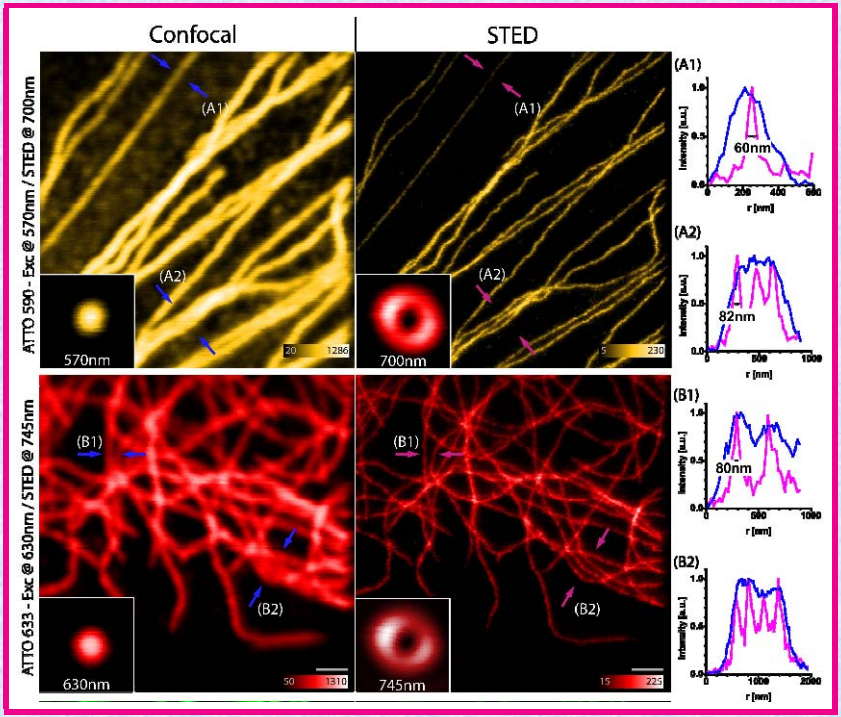

(Wildanger et al., Opt. Exp. **16**, 9614, 2008)

Immunolabeled tubulin fibers imaged at 570 nm and 630 nm.

Optical Coherence Tomography (OCT)

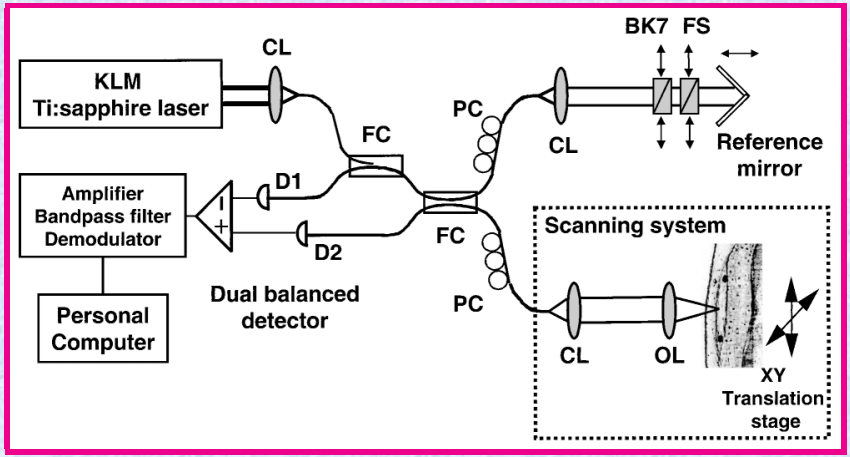

(Drexler et al., Opt. Lett. **24**, 1221, 1999)

- A linear imaging technique based on Michelson interferometry.
- Image resolution ($\Delta z = c\tau_c$) depends on the coherence time τ_c.
- Supercontinuum sources provide a resolution of < 1 μm.

Dual-Band OCT

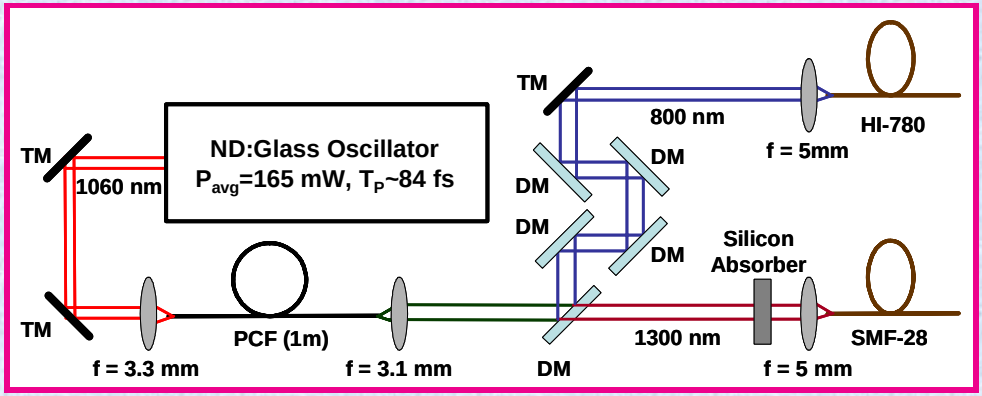

(Fujimoto et al., Opt. Exp. **14**, 1145, 2006)

- OCT is performed simultaneously using two spectral bands located near 800 and 1300 nm.
- Image resolution < 3 μm at 800 and < 5 μm at 1300 nm.
- Combined *in vivo* images of good quality possible.

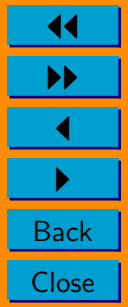

Dual-Band OCT

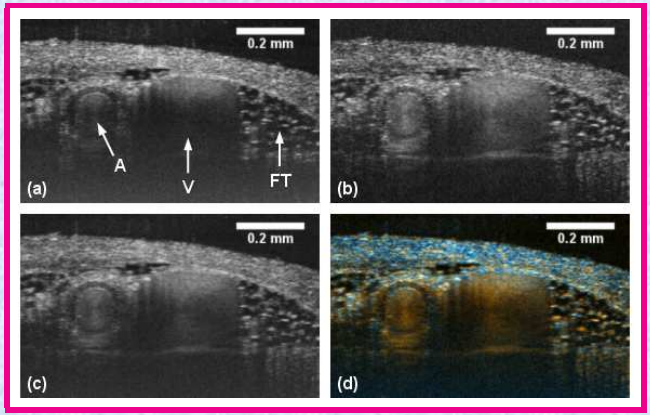

(Cimalla et al., Opt. Exp. **17**, 19486, 2009)

- Simultaneous *in vivo* scans of murine saphenous artery (A), vein (V) and perivascular fat tissue (FT) during the diastole.
- (a) Image at 800 nm; (b) same image at 1250 nm.
- (c) Compounded image of (a) and (b).
- (d) Color-encoded differential image.

High-Resolution OCT

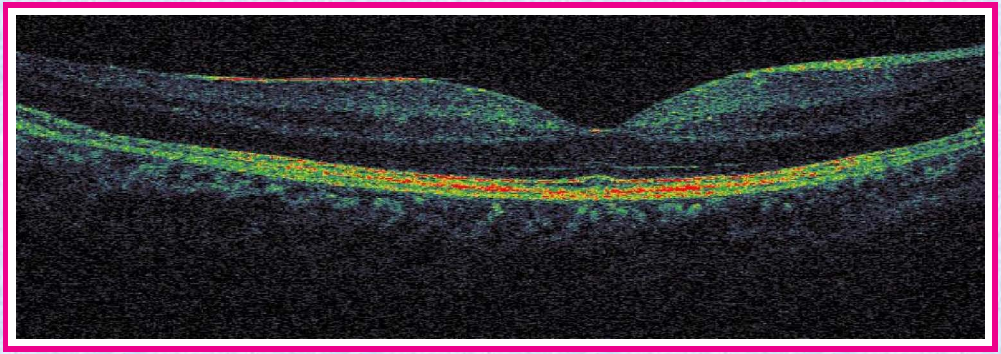

(Nishiura et al., Jap. J. Appl. Phys. **49**, 012701, 2010)

- OCT *in vivo* image of human retina around fovea.
- Observed axial resolution was 2.1 μm in tissue.
- A Gaussian-shape 150-nm-wide supercontinuum was employed for this image.
- OCT is an established medical imaging technique. It is often used to image anterior segment of the eye or the retina.




Back
Close

Concluding Remarks

- Optical fibers were developed during the 1950s and used for biomedical applications during the 1960s.
- They became relevant for telecommunications after 1970 with the development of low-loss fibers.
- By 2000, more than 60 million kilometers of fiber was installed worldwide (on land and in the oceans).
- Biomedical applications of optical fibers are attracting attention in recent years.
- Nonlinear effects in optical fibers make it possible to create a supercontinnum whose bandwidth exceeds 100 THz.
- Such sources are useful for tissue tomography and nonlinear microscopy (biomedical imaging).